

Article

Human Activity Intensity Assessment by Remote Sensing in the Water Source Area of the Middle Route of the South-to-North Water Diversion Project in China

Wenwen Gao ¹, Yuan Zeng ^{1,*}, Yu Liu ² and Bingfang Wu ¹

¹ State Key Laboratory of Remote Sensing Science, Institute of Remote Sensing and Digital Earth, Chinese Academy of Sciences, Beijing 100101, China; gaoww@radi.ac.cn (W.G.); wubf@radi.ac.cn (B.W.)

² Synthesis Research Centre of Chinese Ecosystem Research Network, Key Laboratory of Ecosystem Network Observation and Modelling, Institute of Geographic Sciences and Natural Resources Research, Chinese Academy of Sciences, Beijing 100101, China; liuyu@igsnr.ac.cn

* Correspondence: zengyuan@radi.ac.cn; Tel.: +86-010-6480-6217

Received: 30 July 2019; Accepted: 12 October 2019; Published: 14 October 2019



Abstract: Human activities have significantly affected the natural eco-environment, which could lead to land cover changes. The human activity intensity of land surface (HAILS) represent human activity at the regional scale and can be monitored efficiently over a long term based on land cover data collected by remote sensing techniques. In this study, we quantify the HAILS index for 2000, 2010, and 2015 based on land cover, and analyze its temporal and spatial variation to illustrate the potential influence of human activities on the water quality in the water source area of the Middle Route of the South-to-North Water Diversion Project (MR-SNWDP). The results show that from 2000 to 2015, the HAILS decreased in general but increased with the highest increment of 78.4% around water resources. The area showing high values of HAILS increased at a rate of 30.8% from 2000 to 2015. In the riparian zone around the water body, the HAILS rose at an increment of 0.68% in 2010 to 0.05% in 2015. On the basis of the variation of the HAILS, it has been revealed that human activities, increased mainly around water bodies, may increase the risk of water pollution.

Keywords: human activity intensity; HAILS; remote sensing; the Middle Route of the South-to-North Water Diversion Project

1. Introduction

Since the beginning of human civilization, people have proactively modified and transformed natural ecosystems to acquire valuable natural resources, such as food, fibre, fresh water, etc. [1–7]. As the human population has grown and technology has improved, the scope and nature of human activities has changed drastically worldwide [8–11]. China has a high population density, and the main driver of land cover changes is human activities [12–15]. Changes in land cover can also reveal information on human activities in different ecosystems [16,17]. Therefore, research on human activities is quite important for illustrating ecosystem risks, and monitoring land cover changes can provide a method of illustrating the intensity and type of large-scale human activities, as well as the associated spatial patterns and their temporal and spatial variation.

Nevertheless, due to the comprehensiveness of human activities, quantitative spatial and temporal assessments cannot be performed directly and generally [18,19]. Studies have performed initial estimates of human activities based on comprehensive statistical data [20,21], however, this method cannot assess spatial differences and requires a large amount of socioeconomic statistical data, which is

difficult to obtain during long-term monitoring [22,23]. Currently, indexes of human activity that use quantitative data have been widely used for estimating human activity, and they include the landscape development intensity (LDI) index [24]. In addition, statistical methods that combine geographic and remote sensing data to measure human action types and intensities have also been studied [25], however, the above methods are dependent on ground statistical data, and the study unit is limited to an individual ecological community, which is difficult to apply in large-scale monitoring. The human activity intensity of land surface (HAILS) index was built based on land cover data obtained by remote sensing techniques in 2015, and it reflects human-induced alterations of the natural terrestrial surface, such as water, air, nutrient, and energy exchanges [26]. Compared to the LDI and the above methods, the HAILS shows the direct land cover changes resulting from human activities, reveals changes in human activities explicitly at large or regional scales when adequate socioeconomic data are not available, and takes into account the surface processes of natural environments, such as energy and nutrient exchanges [26].

The construction of infrastructure influences human activities in surrounding areas. China's South-to-North Water Diversion Project (SNWDP) is the largest water diversion project worldwide, and the Middle Route of the SNWDP (MR-SNWDP) diverts drinking water from the Danjiangkou reservoir to northern China [27,28]. In the water source area of the MR-SNWDP, industrial pollution, agricultural fertilizer, urban sewage, and garbage caused by certain human activities have threatened the water quality [29–31]. Although various works have been performed in this study area to monitor ecosystem changes [32–34], studies have not focused on the spatial distribution and variation of human activities as the main factors underlying these ecosystem changes. The objective of this study is to indicate the effect of human activities using the HAILS index and to analyze the spatial patterns and variations of the HAILS to discuss the potential influence of human activities on the water quality in the water source area of the MR-SNWDP.

2. Materials and Methods

2.1. Study Area

The water source area of the MR-SNWDP is located between the latitudes of 31°20'~34°10' N and the longitudes of 106°~112° E. This area is a regional watershed as calculated by a watershed algorithm, and it includes the Danjiangkou reservoir and upper reaches of the Hanjiang River, which is a branch of the Yangtze River, and ranges over the Shaanxi, Henan, Gansu, Sichuan, Hubei, and Chongqing provincial districts (Figure 1). The study area covers 94,500 km² and includes 4 main cities and 47 main counties, which feature a northern subtropical monsoon climate. According to historical records, the mean annual precipitation and temperature are 873.3 mm and 13.71 °C, respectively, and the flood season is from July to September [35]. The geomorphology consists of mountains, hills, mounds, and plains. The area is mainly occupied by natural subtropical evergreen broadleaved forest, deciduous broadleaved forest, and coniferous forest, as well as mixtures of these forests [36].

According to the statistical data for this study area in 2010, the population of the 40 counties amounts to 13.38 million people, and the rural population is approximately 10.65 million, which accounts for 79.65% of the total. The population is mainly distributed around the Danjiangkou reservoir area and along the Han River and the Dan River.

In the water source area of the MR-SNWDP, many governmental policies have been enacted, including the Grain for Green Project in 2001 [37,38], Natural Forest Protection in 2000 [39,40], and the "Danjiangkou reservoir and upstream water pollution control and soil and water conservation planning" launched by the State Council in 2006. With the construction of the MR-SNWDP in 2003, the Danjiangkou reservoir dam height increased from the original 162 m to 176.6 m in 2010 [41]. Ecological migration started with the Grain for Green Project, and policy migration has occurred since 2009 and was completed in 2015, which involved approximately 345,000 people in 6 counties, 40 towns, and 441

villages. Among these people, nearly two-thirds of the immigrants needed to be relocated to 16 new towns [42].

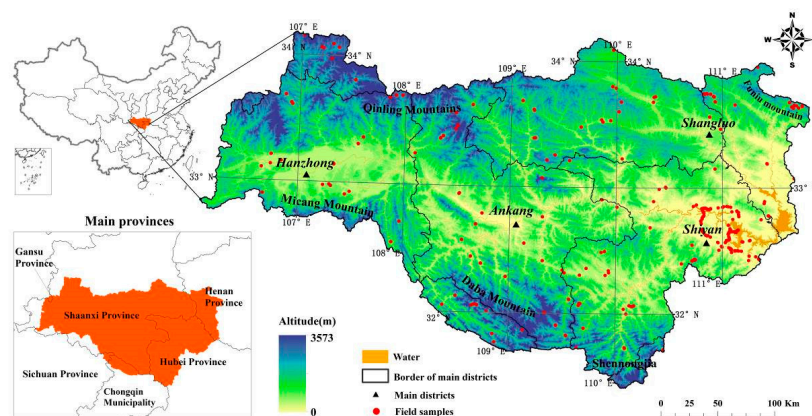


Figure 1. Location of the water source area of the Middle Route of the South-to-North Water Diversion Project (MR-SNWDP) and field sample sites, in 2015.

2.2. Land Cover Classification

We selected HJ-1A/B (HJ) images from May to October in 2000, Landsat TM (TM) images from June to August in 2010 and 2015, as well as a digital elevation model (DEM) from the Advanced Spaceborne Thermal Emission and Reflection Radiometer (ASTER) with a resolution of 30 m. Geometric corrections were conducted in ERDAS IMAGINE 2010 with a root mean square of <1 pixel in the flat areas and <2 pixels in the mountain areas [43]. The classification system, which included forest, shrub, grassland, wetlands, cropland, settlements, and other land types was based on the Land Cover Classification System (LCCS) of the Food and Agriculture Organization of the United Nations (FAO) and considered the characteristics of the study area [44]. An object-based approach was implemented in eCognition 8.0 software and, then, a hierarchical classification was built based on the geometric and texture features of the segmentation objects and several indexes, such as the normalized difference vegetation index, the normalized difference water index, the difference vegetation index, and the ratio vegetation index. In addition, the features of the field samples and empirical classification knowledge were also used as the classification rule set. All of the above methods referred to the ChinaCover classification [45].

Field samples were collected for validation. In 2015, 186 field samples were collected by stratified random sampling (Figure 1). The samples from 2010 and 2000 were selected from Worldview-2 and Google Earth, respectively. The overall accuracy and kappa statistics were adopted for accuracy assessment [46].

2.3. Quantification of Human Activity Intensity

On the basis of the definitions expressed in the HAILS index, different land cover types reflect the various extent of human activities regarding the use, modification, and exploitation of the natural terrestrial surface. Settlement is used as the basic unit, and it is considered the land cover type with the greatest degree of exploitation. The construction land equivalent (CLE) is defined as a basic unit of the equivalent areas of different land cover types. In addition, the conversion index (CI) is the transfer coefficient between the land cover area and its CLE. Table 1 shows the CI value for 7 land cover classes [26]. The HAILS index is defined as follows:

$$HAILS = \frac{S_{CLE}}{S} \times 100\%, \quad (1)$$

$$S_{CLE} = \sum_{i=1}^n (S_{L_i} \times CI_i), \quad (2)$$

where S_{CLE} is the area of CLE , S is the total area, SL_i is the land cover area, CI_i is the transfer coefficient, and n is the class number of the land cover. The units of S_{CLE} , S , and SL_i only need to be unified with no limit, and the HAILS index is a ratio.

Table 1. Conversion index of the construction land equivalent of different land cover types.

Level I Class	Criteria	CI
Forest	natural/semi natural vegetation and artificial vegetation, $H^1 = 3\text{--}30$ m, $C^1 > 20\%$	0
Shrub	natural/semi natural vegetation and artificial vegetation, $H = 0.3\text{--}5$ m, $C > 20\%$	0
Grassland	natural/semi natural vegetation and artificial vegetation, $H = 0.03\text{--}3$ m, $C > 4\%$, water saturation in soil, $K^1 > 0.9$	0.067
Wetland	natural/artificial water, stationary/flowing	0.6
Cropland	artificial vegetation, soil disturbance, crop, harvested	0.2
Settlement	artificial bare surface, settlement, production and services, linear feature, Mining field	1
Other land	Non vegetation, bare rock and soil, $C < 4\%$	0

¹ C is the fractional vegetation cover (%); H is the vegetation height (m); K is the moisture index for grass: $K = r/(0.1Ta)$, where r is the annual rainfall; and Ta is the accumulated daily surface temperature > 0 .

2.4. Spatial and Statistical Analysis Methods

In this study, we calculated the HAILS values in 1.5 km by 1.5 km grids based on the land cover data and divided the data into four levels ($<2\%$, 2% – 10% , 10% – 20% , and $>20\%$). The scale is relatively coarse to match the resolution of the land cover data (30 m), thus making the unit spatial area more homogeneous; however, the scale is finer than that of the population estimates, which may reduce the accuracy of the HAILS index estimation. To balance these issues, 1.5 km by 1.5 km grids might be appropriate, although this size was not rigorously tested in the present study. To analyze the risk of human activities along the flow length distance to the water body, we also divided the study area into 200 buffer belts and classified it into four zones (the riparian zone, valley slope zone, back slope zone, and ridge zone) according to the hydrological path model [47].

We collected data on the agricultural and urban population, population density, gross domestic product (GDP), and production of primary, secondary, and tertiary industry from the yearbooks in the National Library of China, and 47 counties were included in the water source area of the MR-SNWDP in 2010. To assess the relationship between the HAILS index and the above statistical data, Pearson correlations and a multiple regression model were applied [48,49]. In addition, we also calculated the HAILS index in county units to match the statistical data of 47 counties.

The Shiyuan District, where the Danjiangkou reservoir is located, was chosen as an example for analyzing the relationship between the HAILS and chemical fertilizer. The amount of utilized chemical fertilizers, including phosphate and nitrogen fertilizer, was collected from the yearbooks from 1998 to 2007. Based on the fertilizer data, we used the linear regressive equation to predict the fertilizer usage trend [41,50,51].

3. Results

3.1. Land Cover

The land cover changes can be summarized as a continuous decrease in cropland, shrub, grassland, and other land and a significant increase in forest, wetland, and settlement, from 2000 to 2015 (Figure 2). Forest is the main land cover type in the study area. From 2000 to 2010, the area increased by 12,853.2 km², whereas from 2010 to 2015, it showed a slight decrease of approximately 129.9 km². Cropland showed a considerable reduction of 3966.2 km² from 14,529.2 km² in 2000 to 10,563.0 km² in 2010 and then decreased slowly to 10,196.7 km² in 2015. Settlement increased continuously from 608.8 km² in 2000 to 1077.5 km² in 2015. Wetland approximately doubled from 1092.9 km² in 2000 to 2118.9 km² in 2015. Other land, shrub, and grassland all showed significant reductions from 2000 to 2010 and changed slightly from 2010 to 2015. The area of other land types decreased obviously from 293.3 km² in 2000 to 74.4 km² in 2010 and then increased to 74.6 km² in 2015. Shrub reduced considerably by 6503

km² from 2000 to 2010 and increased slightly by 51.5 km² from 2010 to 2015. Grassland decreased from 8884.9 km² in 2000 to 5707.1 km² in 2010, continually decreased to 5668.8 km² in 2015 and showed a slight reduction of 38.3 km² from 2010 to 2015. The overall accuracies are 89.6% in 2000, 87.2% in 2010, and 84.4% in 2015, whereas the kappa statistics (K) are 87.5% in 2000, 83.8% in 2010, and 80.7% in 2015 (Table 2).

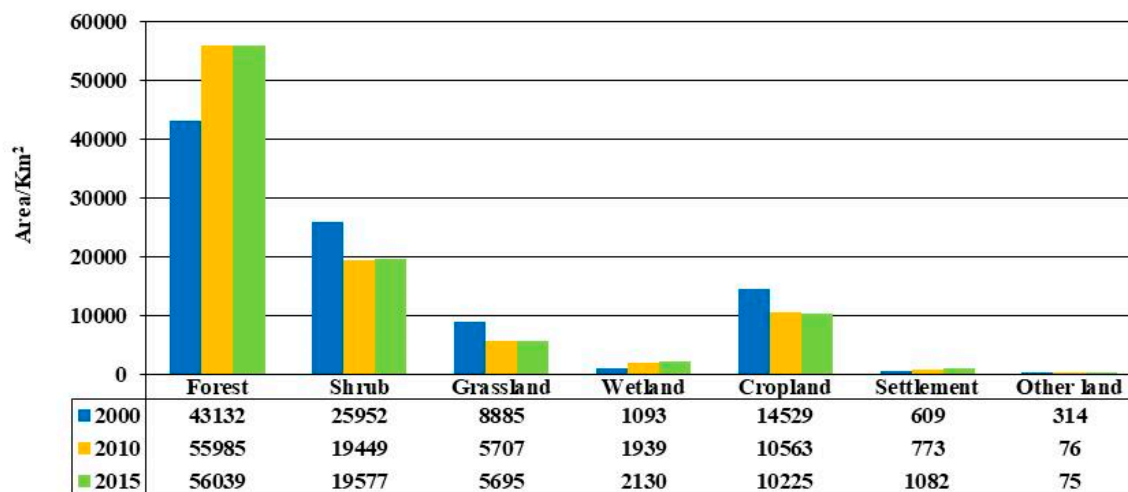


Figure 2. Land cover in 2000, 2010, and 2015.

Table 2. Accuracy of land cover in 2000, 2010, and 2015.

Types	2000			2010			2015		
	Samples	UA (%)	PA (%)	Samples	UA (%)	PA (%)	Samples	UA (%)	PA (%)
Forest	367	94.6	92.0	168	90.5	91.0	36	88.9	88.9
Shrub	211	83.4	85.4	94	83.0	83.0	15	73.3	73.3
Grassland	169	87.6	85.5	53	81.1	78.2	14	71.4	76.9
Wetlands	244	94.3	89.8	113	90.3	93.6	9	88.9	88.9
Cropland	277	89.9	92.6	27	88.9	80.0	11	81.8	81.8
Settlements	588	90.1	93.3	41	85.4	87.5	30	93.3	90.3
Other land	254	82.7	80.5	12	75.0	69.2	7	71.4	71.4
K		87.5			83.8			80.7	
Overall accuracy (%)		89.6			87.2			84.4	

UA, user accuracy and PA, producer accuracy.

3.2. Spatial Pattern of HAILS

In general, the spatial pattern of the HAILS featured high values along the river valley, plains, and hilly areas with gentle landforms in the east and south but low values in the steep mountainous areas. From 2000 to 2015, the HAILS decreased within an area of 60,230.25 km², which accounted for 63.7% of the whole study area, however, the index dramatically increased with the highest increment of 78.4% in the river valley along the tributary of the Han River, as well as in the neighbouring zone of the Danjiangkou reservoir, where the water transfer channel begins (Figure 3).

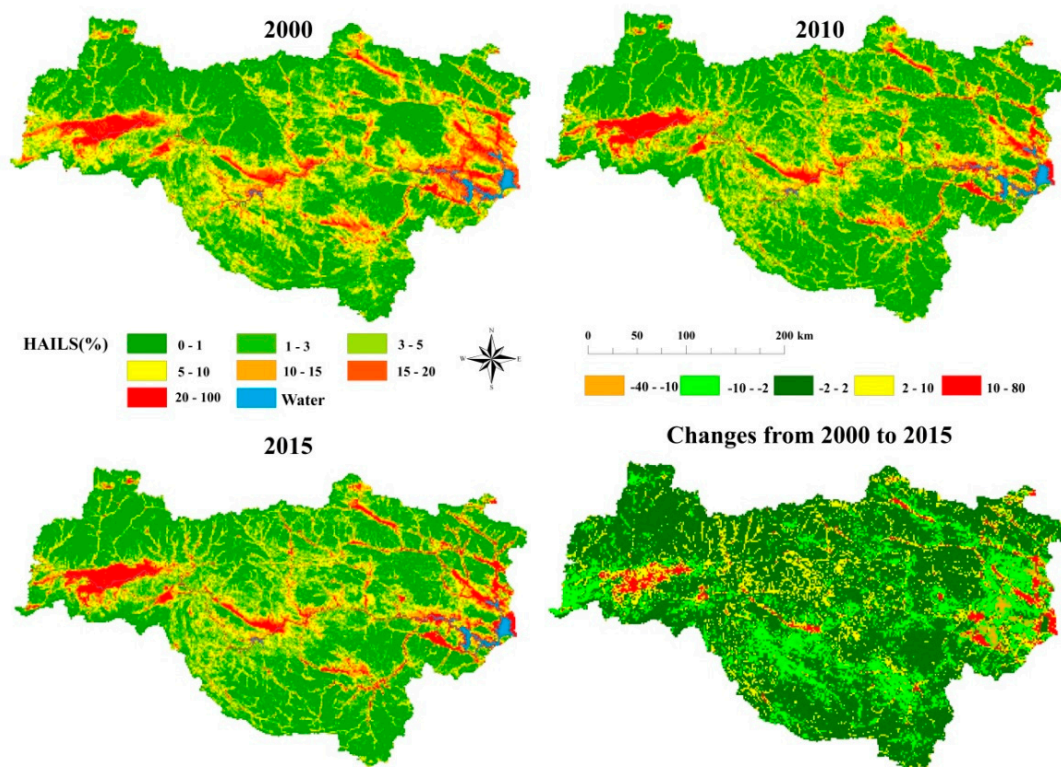


Figure 3. Spatial pattern and changes of the human activity intensity of land surface (HAILS) from 2000 to 2015.

We classified the HAILS into four levels (Table 3). When the HAILS is below 2%, the human activity can be ignored, and the area in this level expanded from 45,291.6 km² to 50,599.0 km². For the level when the HAILS is between 2% and 10%, the area decreased by 2928.1 km², and the mean HAILS also decreased from 4.9% to 4.7%. For the level when the HAILS is from 10% to 20%, the area decreased significantly from 10,875.6 km² in 2000 to 6988.9 km² in 2010 but increased by 121.6 km² from 2010 to 2015. For the level when HAILS is above 20%, the area showed an increasing trend from 2000 to 2015 at a rate of 30.8%, and the mean of the HAILS reached 36.1% in 2015.

Table 3. Grading analysis of HAILS values from 2000 to 2015.

HAILS	<2%		2%–10%		10%–20%		>20%	
	Mean (%)	Area (km ²)						
2000	0.6	45,291.6	4.9	34,000.0	14.4	10,875.6	29.1	4353.5
2010	0.5	50,362.6	4.7	32,233.3	13.9	6988.9	34.4	4928.8
2015	0.5	50,599.0	4.7	31,071.9	13.9	7110.5	36.1	5696.3

3.3. HAILS Variation among Flow-Length Belts

On the basis of the flow-length distance, the following four regions were identified according to the changes of HAILS: The riparian zone (0 to 20 km), valley slope zone (20 to 40 km), back slope zone (40 to 70 km), and ridge zone (70 to 80 km) (Figure 4).

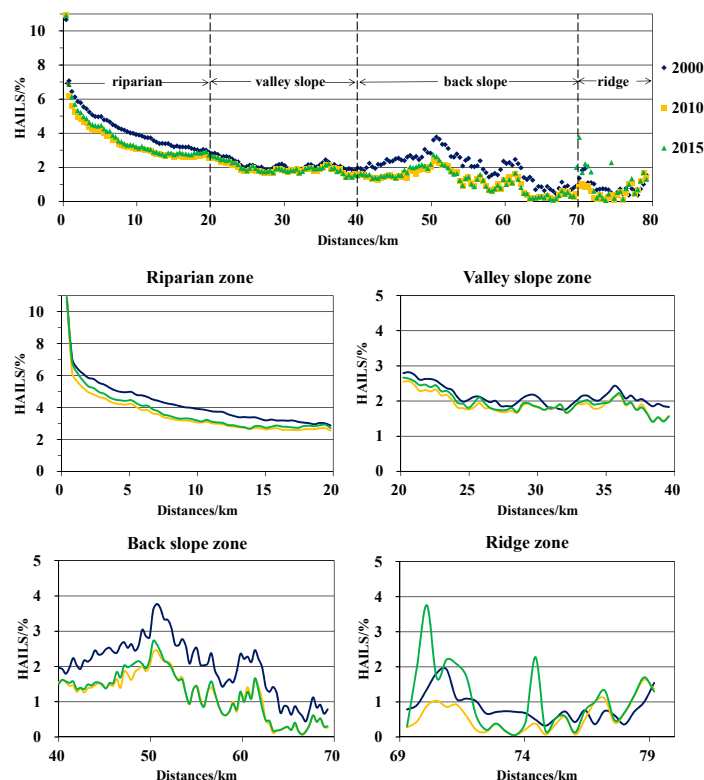


Figure 4. HAILS values in 200 belts divided by the flow-length distance in 2000, 2010, and 2015.

Variations in the HAILS in the four regions indicate different human activity levels from 2000 to 2015. In the riparian zone, the HAILS is between 11% and 2.5% and shows a decreasing trend with distance in 2000, 2010, and 2015. From 2000 to 2010, the HAILS decreased obviously, with the largest decrement of 0.96%, however, from 2010 to 2015, the HAILS increased particularly before 7 km, with an increment from 0.68% to 0.05%. In the valley slope zone, the HAILS showed a slight fluctuation between 1.5% and 2.8%. From 2000 to 2010, the HAILS decreased slightly, with the largest decrement of 0.35%. There seems to be no change from 2010 to 2015, and the largest variation of the HAILS is only 0.08%. The HAILS had apparent fluctuations and decreased slowly, in the back slope zone. An obvious decreasing gap of 1.37% is observed at 51 km from 2000 to 2010, and no changes are observed from 2010 to 2015, except within 48 km to 50 km. In the ridge zone, the HAILS fluctuated heavily. From 2000 to 2010, the HAILS decreased within 70 to 76 km but increased unusually at approximately 0.6% within 76 to 78 km. From 2010 to 2015, the HAILS values all increased, with the lowest increment of 0.02%.

3.4. Relationship between the HAILS and Human Activity

The results of the Pearson correlations show that the seven statistical parameters all had significant correlations with the HAILS (Table 4). The correlation coefficient is the highest between the HAILS and the population density (0.937), which suggests that the HAILS index can generally describe the spatial distribution of the population, production ability, and economic effectiveness. The correlation coefficient of the agricultural population is much higher than that of the urban population, indicating that the HAILS could reflect more details about agricultural activities. Among the three types of industries, primary industry showed the highest correlation coefficient, followed by secondary and tertiary industries.

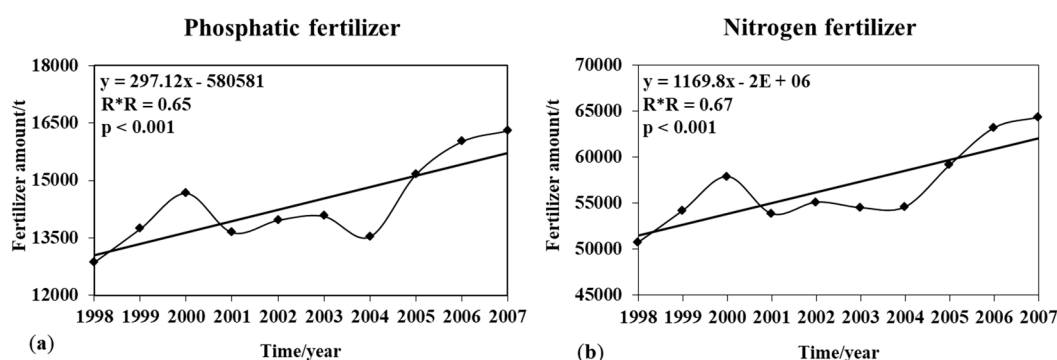
Table 4. Relationship between the HAILS index and statistical data.

HAILS	Population Density	Agricultural Population	Urban Population	GDP	Primary Industry	Secondary Industry	Tertiary Industry
Pearson correlation coefficients	0.937 ***	0.850 ***	0.584 ***	0.765 ***	0.820 ***	0.761 ***	0.619 ***
Multiple regression model coefficients	0.673 ***	0.061 **	0.024 *	−0.348 *	0.188 *	0.363 ***	0.126
VIF	4.801	7.436	4.671	18.411	8.023	6.078	3.130

* p is significant at 10% significance level, ** p is significant at 5% significance level, and *** p is significant at 1% significance level.

Considering the potential multicollinearity problems, we estimated the variance inflation factor (VIF) using a multiple regression model ($R^2 = 0.924$) (Table 4). The results show that the VIF of the GDP is larger than 10, indicating that the GDP has a strong correlation among the six examined statistical parameters [52].

The results of the statistical analysis of phosphate and nitrogen fertilizer are shown in Figure 5. The linear regressive equation showed a positive tendency rate of both phosphate (297.1) and nitrogen (1169.8), which indicated an increasing upward trend. The HAILS values for the Shiyang District are shown in Table 5. From 2000 to 2010, HAILS values below 20% showed a decreasing trend, while high values (>20%) showed an obvious increase, which is associated with the use of chemical fertilizer.

**Figure 5.** Amount of phosphate fertilizer (a) and nitrogen fertilizer (b) utilized in the Shiyang District.**Table 5.** Grading analysis of the HAILS in the Shiyang District.

Mean HAILS (%)	<2%	2%–10%	10%–20%	>20%
2000	0.8	5.1	14.4	29.1
2010	0.5	4.9	13.8	36.5

4. Discussion

4.1. Effectiveness of HAILS

Primary industry refers to agriculture and animal husbandry [53]; secondary industry includes mining, manufacturing, energy supply, as well as construction [54]; and tertiary industry involves transportation, warehousing, postal services, information transmission, and other service aspects [55]. According to the definition in the HAILS index, construction and agricultural land accounted for the greatest proportion in the calculations. Primary and secondary industry can significantly affect natural properties via reclaiming, cultivating, fertilizing, and building on artificial surfaces. These actions modify and even exploit the original natural environment, whereas vegetation land surfaces are only utilized without changes to their natural properties, as is the case with grassland and forest. Thus, the HAILS index better describes human activities associated with agricultural and construction land.

Previous studies have found that human activity is a key factor affecting water quality [56–58]. The main human activities that impact the water quality include agricultural and urban activities,

which consider the sewage generated in urban areas and the use of fertilizers, especially on cultivated land along rivers [59]. In the study area, agricultural nonpoint pollution was an important factor that affected the water quality [60]. From 2001 to 2005, agricultural activities caused significant water pollution around the Danjiangkou reservoir [61], and the water quality was still poor from 2011 to 2015, which was affected by both agricultural and urban activities [62]. In the Shiyan District, as the cropland area was decreased by construction activities [63], the increased use of chemical fertilizer resulted in an increase of pollutants per arable land unit, and these pollutants might be transported in the surface runoff and cause subsequent water pollution [64]. The HAILS index showed the same increasing trend from 2000 to 2010, as well. Therefore, the HAILS index can reflect the influence on the water quality indirectly.

The four levels of HAILS statistical data and four zones classified by the flow-length distance are suitable for human activity analyses in this study area, which has a northern subtropical monsoon climate, however, in regions with a single land cover type and different climate environments, the use of the HAILS index for human activity assessments would probably be restricted. A quantitative estimation of human activity still needs to combine more statistics on the ground conditions obtained via remote sensing data to clearly illustrate the relationship between the output of human production and the pollution input from human activities.

4.2. Impacts of Human Activity

This study reveals multiple changes of human activities in the water source area of the MR-SNWDP. These changes are mainly caused by policy implementation, economic development, and topography. The government started the Grain for Green Project in 1999 (GGP) and Natural Forest Protection (NFP) in 2000 to relieve soil erosion and land desertification, limit the felling of trees, and rehabilitate vegetation growing in the main natural forest areas [4,65,66]. After the construction of the MR-SNWDP in 2003, local conservation policies, such as the Water Pollution Control, Soil, and Water Conservation Plan, were implemented and focused on water conservation in the back slope zone, which is the most suitable zone for cropping. In addition, the immigration plan started in 2010, with nearly 236 thousand immigrants relocated to 16 new towns, which were almost all located in mountainous areas [67,68], and therefore variations in the HAILS in the back slope zone show that human activity obviously decreased due to cutting back the poverty introduced by emigrating people, in the steep mountainous regions [69].

The Western Development Plan implemented in 2000 and the Rise of Central China Plan implemented in 2004 improved the regional economy and employed an incentive-based approach with payments. The economic improvements and increased population promoted the demand for food, housing, working, industrial buildings, and transportation facilities [70], which resulted in the increase of the HAILS index in the riparian zones and neighbouring reservoir areas. In addition, these changes resulted in the immigration of a high percentage of the agricultural population in mountain regions to cities and counties. In the back slope zone, movement of the agricultural population, subsequently, influenced the populations' livelihoods and attitudes towards the environment, which promoted ecosystem recovery and resulted in a decrease of the HAILS [37].

Due to topographic limitations, the valley slope zone is unsuitable for cultivation and is on a restoration track, which has resulted in continuous decreases of human activity over the past 15 years. The ridge zone is heavily influenced by the tourism industry. In Zhashui County of the Shangluo District, new roads, resorts, pagodas, and other buildings were constructed over a period of five years [71]. However, the ridge zone accounts for a small area and is far away from water resources, and the sensitive and fragile nature of the ecological system makes it difficult for the area to recover once damaged.

5. Conclusions

Within 15 years, significant changes have occurred according to variations in the HAILS index. The results indicate high values for the HAILS along river valleys, plains, and hilly areas that present gentle landforms in the east and south but low values in the steep mountainous areas. From 2000 to 2015, the HAILS decreased across 63.7% of the study area but increased with the highest increment of 78.4% in the river valley along the tributary of the Han River and around the Danjiangkou reservoir. When the HAILS was classified as above 20%, the area showed an increasing rate of 30.8%, and the mean HAILS value reached 36.1% in 2015.

The variations of the HAILS in the four zones indicate that different management and development practices are needed. On the basis of the flow length distance, the HAILS index in the valley slope zone and back slope zone both decreased from 2000 to 2015. The valley slope zone is unsuitable for cultivation due to topographic limitations and the back slope zone is usually well protected by governmental policies, however, in the riparian zone, which is located close to water, the HAILS was between 11% and 2.5%, and from 2010 to 2015, the HAILS values increased, particularly within 7 km, and the increment was from 0.68% to 0.05%. Thus, the riparian zone can be considered a sensitive region for water resource protection.

This study focused on the water source area of the MR-SNWDP, where water quality is the focus of significant attention because the water from this area is delivered to North China. Variations in the human activity intensity may affect the hydrological environment and diminish the water quality, which is an effect that can be observed based on changes in the HAILS, especially in the riparian zone. To further detect the relationship between human activity and hydrological environments, we plan to try to collect water quality data from relevant departments. In addition, remote sensing techniques can be broadly applied in ecological research. Therefore, methods of combining ecology parameters and remote sensing techniques must be developed to improve assessments of variations in human activity intensity and protect ecosystems.

Author Contributions: Conceptualization, W.G. and Y.L.; data curation, W.G.; formal analysis, W.G.; funding acquisition, Y.Z. and B.W.; methodology, W.G.; project administration, Y.Z. and B.W.; supervision, Y.Z. and B.W.; Writing—Original Draft, W.G.; Writing—Review and Editing, Y.Z. and B.W.

Funding: This research was funded by the National Key Research and Development Program of China (No. 2016YFC0502102-02), the National Natural Science Foundation of China (No. 41671365, 41771464), and the annual project from the Research Center for Policy and Technology of the Office of the South-to-North Water Diversion Project, Ministry of Water Resources (No. 2018-21).

Acknowledgments: We greatly appreciate the project cooperation provided by Zhimin Wang, Yuanshu Liu, Zhiyuan Ren, Pengfei Cao, Kun Hou, Lingguang Meng, and Guiquan Hu. We thank Yujin Zhao and Dan Zhao for their assistance with the field sample collection. We also thank Xinfeng Zhao and Zhaouju Zheng for the technological help.

Conflicts of Interest: The authors declare no conflict of interest.

References

1. De Groot, R.S.; Wilson, M.A.; Boumans, R.M.J. A typology for the classification, description and valuation of ecosystem functions, goods and services. *Ecol. Econ.* **2002**, *41*, 393–408. [[CrossRef](#)]
2. Faber, J.H.; Van Wensem, J. Elaborations on the use of the ecosystem services concept for application in ecological risk assessment for soils. *Sci. Total Environ.* **2012**, *415*, 3–8. [[CrossRef](#)] [[PubMed](#)]
3. Klein Goldewijk, K.; Ramankutty, N. Land cover change over the last three centuries due to human activities: The availability of new global data sets. *GeoJournal* **2004**, *61*, 335–344. [[CrossRef](#)]
4. Ouyang, Z.; Zheng, H.; Polasky, S.; Liu, J.; Xu, W.; Wang, Q.; Zhang, L.; Xiao, Y.; Rao, E.; Jiang, L.; et al. Improvements in ecosystem services from investments in natural capital. *Science* **2016**, *352*, 1455–1459. [[CrossRef](#)] [[PubMed](#)]
5. Seaquist, J.W.; Hickler, T.; Eklundh, L.; Ardö, J.; Heumann, B.W. Disentangling the effects of climate and people on Sahel vegetation dynamics. *Biogeosciences* **2009**, *6*, 469–477. [[CrossRef](#)]

6. Vitousek, P.M.; Lubchenco, J.; Melillo, J.M.; Mooney, H.A. Human domination of earth's ecosystems. *Science* **1997**, *277*, 494–499. [[CrossRef](#)]
7. Wessels, K.J.; Prince, S.D.; Frost, P.E.; Van Zyl, D. Assessing the effects of human-induced land degradation in the former homelands of northern South Africa with a 1 km AVHRR NDVI time-series. *Remote Sens. Environ.* **2004**, *91*, 47–67. [[CrossRef](#)]
8. Gleckler, P.J.; Santer, B.D.; Domingues, C.M.; Pierce, D.W.; Barnett, T.P.; Church, J.A.; Taylor, K.E.; AchutaRao, K.M.; Boyer, T.P.; Ishii, M.; et al. Human-induced global ocean warming on multidecadal timescales. *Nat. Clim. Chang.* **2012**, *2*, 524–529. [[CrossRef](#)]
9. Zhao, C.; Shao, N.; Yang, S.; Ren, H.; Ge, Y.; Zhang, Z.; Feng, P.; Liu, W. Quantitative assessment of the effects of human activities on phytoplankton communities in lakes and reservoirs. *Sci. Total Environ.* **2019**, *665*, 213–225. [[CrossRef](#)]
10. Mouri, G. Assessment of land cover relocation incorporating the effects of human activity in typical urban and rural catchments for the design of management policies. *Environ. Sci. Policy* **2015**, *50*, 74–87. [[CrossRef](#)]
11. Syvitski, J.P.M.; Kettner, A.J.; Overeem, I.; Hutton, E.W.H.; Hannon, M.T.; Brakenridge, G.R.; Day, J.; Vörösmarty, C.; Saito, Y.; Giosan, L.; et al. Sinking deltas due to human activities. *Nat. Geosci.* **2009**, *2*, 681–686. [[CrossRef](#)]
12. Cao, Z.; Duan, H.; Feng, L.; Ma, R.; Xue, K. Climate- and human-induced changes in suspended particulate matter over Lake Hongze on short and long timescales. *Remote Sens. Environ.* **2017**, *192*, 98–113. [[CrossRef](#)]
13. Valipour, M. Land use policy and agricultural water management of the previous half of century in Africa. *Appl. Water Sci.* **2015**, 367–395. [[CrossRef](#)]
14. Mariano, D.A.; dos Santos, C.A.C.; Wardlowa, B.D.; Anderson, M.C.; Schiltmeyer, A.V.; Tadesse, T.; Svoboda, M.D. Use of remote sensing indicators to assess effects of drought and human-induced land degradation on ecosystem health in Northeastern Brazil. *Remote Sens. Environ.* **2018**, *213*, 129–143. [[CrossRef](#)]
15. Wang, T.; Sun, J.; Han, H.; Yan, C. The relative role of climate change and human activities in the desertification process in Yulin region of northwest China. *Environ. Monit. Assess.* **2011**, *184*, 7165–7173. [[CrossRef](#)]
16. Song, W.; Deng, X. Land-use/land-cover change and ecosystem service provision in China. *Sci. Total Environ.* **2017**, *576*, 705–719. [[CrossRef](#)]
17. Zhang, Y.; Zhang, C.; Wang, Z.; Chen, Y.; Gang, C.; An, R.; Li, J. Vegetation dynamics and its driving forces from climate change and human activities in the Three-River Source Region, China from 1982 to 2012. *Sci. Total Environ.* **2016**, *563–564*, 210–220. [[CrossRef](#)]
18. Zang, Z.; Zou, X.; Song, Q.; Yao, Y. Analysis of the spatiotemporal correlation between vegetation pattern and human activity intensity in Yancheng coastal wetland, China. *Anthr. Coasts* **2019**, *2*, 87–100. [[CrossRef](#)]
19. Gao, Z.J.; Wu, C.L. Quantitative Assessment of Urban Human Activity Intensity Based on GIS-A Case Study of the Pearl River Delta. In Proceedings of the International Conference on Geoinformatics, Beijing, China, 18 June 2010.
20. Liu, S.H.; Prieler, S.; Li, X.B. Spatial patterns of urban land use growth in Beijing. *J. Geogr. Sci.* **2002**, *12*, 266–274. [[CrossRef](#)]
21. Zhang, G.Y.; Wang, Z. Quantitative assessment of human activity intensity in the Heihe catchment. *Adv. Earth Sci.* **2004**, *19*, 386–390. [[CrossRef](#)]
22. Wang, J.Z.; Zhang, G.H.; Nie, Z.L.; Yan, M.J. Quantitative assessment of human activity intensity in Hutuohe catchment. *J. Arid Land Resour. Environ.* **2009**, *23*, 41–44. [[CrossRef](#)]
23. Dai, Z.X.; Guldmann, J.M.; Hu, Y.F. Spatial regression models of park and land-use impacts on the urban heat island in central Beijing. *Sci. Total Environ.* **2018**, *626*, 1136–1147. [[CrossRef](#)] [[PubMed](#)]
24. Brown, M.T.; Vivas, M.B. Landscape development intensity index. *Environ. Monit. Assess.* **2005**, *101*, 289–309. [[CrossRef](#)] [[PubMed](#)]
25. Terra, T.N.; Dos Santos, R.F. Measuring cumulative effects in a fragmented landscape. *Ecol. Model.* **2012**, *228*, 89–95. [[CrossRef](#)]
26. Xu, Y.; Xiaoyi, S.; Tang, Q. Human activity intensity of land surface: Concept, method and application in China. *J. Geogr. Sci.* **2015**, *70*, 1068–1079. [[CrossRef](#)]
27. Dong, Z.; Yan, Y.; Duan, J.; Fu, X.; Zhou, Q.; Huang, X.; Zhu, X.; Zhao, J. Computing payment for ecosystem services in watersheds: An analysis of the Middle Route Project of South-to-North Water Diversion in China. *J. Environ. Sci.* **2011**, *23*, 2005–2012. [[CrossRef](#)]

28. Li, S.; Li, J.; Zhang, Q. Water quality assessment in the rivers along the water conveyance system of the Middle Route of the South to North Water Transfer Project (China) using multivariate statistical techniques and receptor modeling. *J. Hazard. Mater.* **2011**, *195*, 306–317. [[CrossRef](#)]
29. Li, S.; Gu, S.; Tan, X.; Zhang, Q. Water quality in the upper Han River basin, China: The impacts of land use/land cover in riparian buffer zone. *J. Hazard. Mater.* **2009**, *165*, 317–324. [[CrossRef](#)]
30. Li, W.; Zeng, Y.; Zhang, L.; Yin, K.; Yuan, C.; Wu, B. The spatial pattern of landcover in the drawdown area of Danjiangkou reservoir. *Remote Sens. Land Resour.* **2011**, *91*, 108–114. [[CrossRef](#)]
31. Zhou, Z.; Zeng, Y.; Zhang, L.; Du, X.; Wu, B. Remote Sensing monitoring and analysis of fractional vegetation cover in the Water Source Area of the Middle Route of Projects to Divert Water from South to North. *Remote Sens. Land Resour.* **2012**, *92*, 70–76. [[CrossRef](#)]
32. Chen, H.C.; Du, P. Potential ecological benefits of the Middle Route for the South-North Water Diversion Project. *Tsinghua Sci. Technol.* **2008**, *13*, 715–719. [[CrossRef](#)]
33. Duan, Z.; Zhang, L.; Li, L. The extreme precipitation change characteristics of the source area of the middle route of South-North Water Transfer Project. *Procedia Eng.* **2012**, *28*, 569–573. [[CrossRef](#)]
34. Li, S.; Cheng, X.; Xu, Z.; Han, H.; Zhang, Q. Spatial and temporal patterns of the water quality in the Danjiangkou reservoir, China. *Hydrol. Sci. J.* **2009**, *54*, 124–134. [[CrossRef](#)]
35. Wang, L.; Ma, C. A study on the environmental geology of the Middle Route Project of the South-North water transfer. *Eng. Geol.* **1999**, *51*, 153–165. [[CrossRef](#)]
36. Ren, Z.Y.; Zhang, Y.F.; Li, J. The value of vegetation ecosystem services: A case of Qinling-Daba Mountains. *J. Geogr. Sci.* **2003**, *13*, 195–200. [[CrossRef](#)]
37. Lu, Q.; Xu, B.; Liang, F.; Gao, Z.; Ning, J. Influences of the Grain-for-Green project on grain security in southern China. *Ecol. Indic.* **2013**, *34*, 616–622. [[CrossRef](#)]
38. Zhou, D.; Zhao, S.; Zhu, C. The grain for green project induced land cover change in the Loess Plateau: A case study with Ansai County, Shanxi Province, China. *Ecol. Indic.* **2012**, *23*, 88–94. [[CrossRef](#)]
39. Shen, Y.Q.; Liao, X.C.; Yin, R.S. Measuring the socioeconomic impacts of China's Natural Forest Protection Program. *Environ. Dev. Econ.* **2006**, *11*, 769–788. [[CrossRef](#)]
40. Ren, G.-P.; Young, S.S.; Wang, L.; Wang, W.; Long, Y.; Wu, R.; Li, J.; Zhu, J.; Yu, D.W. Effectiveness of China's National Forest Protection Program and nature reserves. *Conserv. Biol.* **2015**, *29*, 1368–1377. [[CrossRef](#)]
41. Yu, P.; Yang, T.; Wu, C. Impact of climate change on water resources in southern Taiwan. *J. Hydrol.* **2002**, *260*, 161–175. [[CrossRef](#)]
42. Zhang, Q. The South-to-North Water Transfer Project of China: Environmental implications and monitoring strategy. *J. Am. Water Resour. Assoc.* **2009**, *45*, 1238–1247. [[CrossRef](#)]
43. Richter, R. Correction of satellite imagery over mountainous terrain. *Appl. Opt.* **1998**, *37*, 4004. [[CrossRef](#)] [[PubMed](#)]
44. Zhang, L.; Li, X.; Yuan, Q.; Liu, Y. Object-based approach to national land cover mapping using HJ satellite imagery. *J. Appl. Remote Sens.* **2014**, *8*, 83686. [[CrossRef](#)]
45. Wu, B.; Qian, J.; Zeng, Y.; Zhang, L.; Yan, C.; Wang, Z.; Li, A.; Ma, R.; Yu, X.; Huang, J.; et al. *Land Cover Atlas of the People's Republic of China (1:1,000,000)*, 1st ed.; Sinomaps Press: Beijing, China, 2017; pp. 254–261.
46. Sim, J.; Wright, C.C. The kappa statistic in reliability studies: Use, interpretation, and sample size requirements. *Phys. Ther.* **2005**, *85*, 257–268. [[CrossRef](#)] [[PubMed](#)]
47. Hickey, R. Slope angle and slope length solutions for GIS. *Cartography* **2000**, *29*, 1–8. [[CrossRef](#)]
48. Li, Y.; Li, H.; Liu, Z.; Miao, C. Spatial Assessment of Cancer Incidences and the Risks of Industrial Wastewater Emission in China. *Sustainability* **2016**, *8*, 480. [[CrossRef](#)]
49. Li, H.; Li, Y.; Lee, M.-K.; Liu, Z.; Miao, C. Spatiotemporal Analysis of Heavy Metal Water Pollution in Transitional China. *Sustainability* **2015**, *7*, 9067–9087. [[CrossRef](#)]
50. Jang, D.; Lim, D.; Chae, G.; Yoo, J. A novel algorithm based on the coefficient of determination of linear regression fitting to automatically find the optimum angle for miniaturized surface plasmon resonance measurement. *Sens. Actuators B Chem.* **2014**, *199*, 488–492. [[CrossRef](#)]
51. Usevich, K.; Markovsky, I. Adjusted least squares fitting of algebraic hypersurfaces. *Linear Algebra Appl.* **2016**, *502*, 243–274. [[CrossRef](#)]
52. Chatterjee, S.; Hadi, A.S. *Regression Analysis by Example*; John Wiley & Sons: New York, NY, USA, 2013.

53. Curt, H.S. The influence of secondary production on industry definition in the extended vertical market model. *Strateg. Manag. J.* **1992**, *13*, 171–187. Available online: <https://www.jstor.org/stable/2486383> (accessed on 12 October 2019).
54. Zhu, G.; Xiao, Y.; Wan, C. The study of indicator framework of Cleaner Production in the tertiary industry. *Appl. Mech. Mater.* **2013**, *295–298*, 759–762. [[CrossRef](#)]
55. Xie, W.J.; Gu, G.F.; Zhou, W.X. On the growth of primary industry and population of China's counties. *Phys. A Stat. Mech. Appl.* **2010**, *389*, 3876–3882. [[CrossRef](#)]
56. Mancini, L.; Marcheggiani, S.; Puccinelli, C.; Lacchetti, I.; Carere, M. Global environmental changes and the impact on ecosystems and human health. *Energy Environ. Innov.* **2017**, *3*, 98–104. [[CrossRef](#)]
57. Anderson, D.M.; Glibert, P.M.; Burkholder, J.M. Harmful algal blooms and eutrophication: Nutrient sources, composition, and consequences. *Estuaries* **2002**, *25*, 704–726. [[CrossRef](#)]
58. Davraza, A.; Senerb, E.; Sener, S. Evaluation of climate and human effects on the hydrology and water quality of Burdur Lake, Turkey. *J. Afr. Earth Sci.* **2019**, *158*, 103569. [[CrossRef](#)]
59. Tian, Y.; Jiang, Y.; Liu, Q.; Dong, M.; Xu, D.; Liu, Y.; Xu, X. Using a water quality index to assess the water quality of the upper and middle streams of the Luanhe River, northern China. *Sci. Total Environ.* **2019**, *667*, 142–151. [[CrossRef](#)]
60. Du, Y.; Tang, R.; Dang, X.; Hu, Y.; Zhu, S.; Meng, M. Evaluation for the water quality of drinking water source of Shiyuan urban area in Hubei province. *Environ. Prot.* **2016**, *22*, 34–37.
61. Li, S.; Zhang, Q. Assessing the Water Quality in the Water Source Area of the Middle Route of the South to North Water Transfer Project (Danjiangkou Reservoir) Using A Water Quality Index Method. *Res. Environ. Sci.* **2008**, *22*, 61–68. [[CrossRef](#)]
62. Shi, J.; Yin, Y.; Wang, M.; Deng, L.; Huang, J.; Chen, H.; Du, Z.; Zhang, Y.; Li, Y. Water Quality Analysis of Danjiang Reservoir before and after Running of the Mid-line Project of South to North Water Diversion. *J. Hunan Univ. Sci. Technol.* **2018**, *33*, 103–109. [[CrossRef](#)]
63. Gao, W.; Zeng, Y.; Zhao, D.; Wu, B.; Ren, Z. Land cover changes and drivers in the water source area of the Middle Route of the South-to-North Water Diversion Project in China from 2000 to 2015. *Chin. Geogr. Sci.* in press.
64. Salvettia, R.; Acutisb, M.; Azzellinoa, A.; Carpani, M.; Giupponi, C.; Parati, P.; Vale, M.; Vismara, R. Modelling the point and non-point nitrogen loads to the Venice Lagoon (Italy): The application of water quality models to the Dese-Zero basin. *Desalination* **2008**, *226*, 81–88. [[CrossRef](#)]
65. Chi, W.F.; Zhao, Y.Y.; Kuang, W.H.; He, H.L. Impacts of anthropogenic land use/cover changes on soil wind erosion in China. *Sci. Total Environ.* **2019**, *668*, 204–215. [[CrossRef](#)] [[PubMed](#)]
66. Zhang, Q.; Xu, Z.; Shen, Z.; Li, S.; Wang, S. The Han River watershed management initiative for the South-to-North Water Transfer Project (Middle Route) of China. *Environ. Monit. Assess.* **2009**, *148*, 369–377. [[CrossRef](#)] [[PubMed](#)]
67. Johnson, D.G. Provincial migration in China in the 1990s. *China Econ. Rev.* **2003**, *14*, 22–31. [[CrossRef](#)]
68. Wang, Y.; Guo, S.; Yang, G.; Hong, X.; Hu, T. Optimal early refill rules for Danjiangkou Reservoir. *Water Sci. Eng.* **2014**, *7*, 403–419. [[CrossRef](#)]
69. Feng, Q.; Chen, J. Sustainable Development of Natural Forest Protection Project Area. *J. Beijing For. Univ.* **2009**, *8*, 28–31. [[CrossRef](#)]
70. Lü, Y.; Zhang, L.; Feng, X.; Zeng, Y.; Fu, B.; Yao, X.; Li, J.; Wu, B. Recent ecological transitions in China: Greening, browning, and influential factors. *Sci. Rep.* **2015**, *5*, 8732. [[CrossRef](#)]
71. Zhang, Y. Distribution and evaluation of ecological tourism resources in Shangluo City. *Acta Agric. Jiangxi* **2011**, *23*, 165–166.

